MACROKINETICS OF AN AUTOWAVE MODE OF SYNTHESIS OF ORGANIC POWDERS IN A CONDENSED PHASE. 1. DYNAMIC INVESTIGATIONS OF SELF-PROPAGATING SYNTHESIS OF ORGANIC POWDERS IN A CONDENSED PHASE

A. D. Ubortsev, B. M. Khusid, Z. P. Shul'man, A. G. Merzhanov, and V. A. Mansurov

UDC 536.46.524:541.128

A comparison is made between the autowave processes of self-propagating high-temperature synthesis (SHS), combustion of pyrotechnic compositions, and self-propagating synthesis in organic mixtures. It is shown that autowave modes in organic mixtures involve a variation in the electrophysical properties of a composition. Studying the latter allows one to determine the stages of microkinetic transformations based on the results of dynamic investigations of the self-propagating synthesis.

Introduction. The current study considers physicochemical transformations in heterogeneous condensed media, proceeding with an autowave propagation mode of exothermal reactions in the mixtures of organic powders. A highly promising process is the self-propagating high-temperature synthesis with the following distinctive features, viz., short times of synthesis, insignificant external energy expenditure, simplicity of equipment, and high efficiency and flexibility. The propagation rate of the wave, as well as its shape and amplitude are independent of initial conditions in a fairly wide range, but are instead governed by local characteristics of the medium proper. Utilization of the heat liberated during synthesis, along with the above-mentioned distinctive features, testifies to the great advantages of this process from the technological standpoint. Self-propagating synthesis in organic systems, discovered in [1], opens up new potentials both for organic chemistry and for the SHS method.

The results obtained permit us to remark that, during the product synthesis, no solvent is required at any stage, and the products are easily treated mechanically. Furthermore, self-propagating synthesis in organic systems involves crystallization, which promotes self-purification of the forming product. To effect SHS, at the outset of the process a wave mode is initiated by a thermal pulse, with which structural and physicochemical transformations are centered in the zone, moving over a heterogeneous mixture of solids [2]. It is essential and helpful to study self-propagating synthesis in mixtures of organic powders because of the following trends [1]:

1) possibilities of setting up the technology for producing new nontraditional organic materials based on self-propagating synthesis;

2) use of organic systems for studying autowave processes in the condensed phase.

The conditions for implementing self-propagating synthesis in organic systems (T = 100-300°C and combustion rate about 1 mm/sec) enable an extension of the ranges of properties and effects associated with SHS.

Table 1 gives the results of comparing SHS [3-6], the combustion of pyrotechnic compositions on the basis of organic compounds [7-11], and self-propagating synthesis in the condensed phase in mixtures of organic powders [1, 12-14]. The processes occurring in familiar mixtures of organic powders are similar to autowave exothermal reactions, proceeding in the condensed phase in inorganic mixtures.

A. V. Lykov Heat and Mass Transfer Institute of the Academy of Sciences of Belarus, Minsk. Institute of Structural Macrokinetics of the Russian Academy of Sciences, Chernogolovka. Translated from Inzhenerno-Fizicheskii Zhurnal, Vol. 63, No. 2, pp. 131-139, August, 1992. Original article submitted October 17, 1991.

1062-0125/92/6302-0749$12.50

TABLE 1. Results of Comparing Autowave Processes

Q_g/RT_g	T_g/T_p	Q_g/RT_p	Autowave processes
0,05—0,2	0,6—1,1	0,04—0,3	SHS
0,12—0,4	1,5—5	2,4—6	in pyrotechnic compositions
0,15—0,19	0,7—0,9	0,1—0,3	in organic powders

Note. Q_g is the thermal effect, T_g is the maximal temperature of combustion, and T_p is the melting temperature of original components.

The combustion wave for gun powders and explosives is associated with an abrupt fall of density (evaporation and gasification). These distinctions are especially vivid at the depression stage following rapid combustion of the heated layer. The heat influx from the gaseous zone of the reaction products is relatively small. The high density of thermal energy in the condensed products allows efficient maintenance of the combustion front during depression.

Thus, the study of exothermal frontal reactions in the condensed phase in mixtures of organic powders will demonstrate the possibility of applying SHS technologies for producing organic materials [15].

Consideration is given to self-propagating synthesis in reactions between malonic acid ($C_3H_4O_4$) and piperazine ($C_4H_{10}N_2$), which are colorless crystals with melting points of 136 and 112°C, respectively. During synthesis, a salt of malonic acid and piperazine forms, which is a crystalline substance with a melting point of 180°C. Studies [1, 4] shows that in the given system gas-free combustion with a 100% product yield occurs. The product was identified using NMR, x-ray diffraction analysis, and IR spectroscopy. These works have established the dependences of the rate, maximal temperature in the front, and quantity of undercombustion on the particle size and molar ratio of components, derived from measurements by two thermocouples.

The primary focus is on the dynamic investigation of the processes of gas-free combustion in a stoichiometric mixture of malonic acid and piperazine.

Investigation Technique. For experimental investigations of the given processes we used a setup consisting of a reactor, a matrix of temperature and electrochemical probes, and an automated system for scientific studies based on the IVK-6 complex. Unlike the traditional methods of contact thermometry [1, 2, 4-6], the presented design of probes permits measurements of spatial–temporal temperature distributions, electric conductivity, and potential difference in the reactor in real time.

The synthesis processes are performed in a cylindrical reactor made of quartz glass (Fig. 1a). Because of the high hygroscopicity of the reagents it was placed in an atmosphere of desiccated high-purity argon. Preliminary tests established the critical diameter of the reactor, equal to 15 mm. The prepared original mixture was heated by a flat Nichrome spiral, with a short pulse of 10 sec, up to a temperature of 200°C. The measurements were performed on the sections with the front velocity stabilized and independent of the ignition conditions. A sensor (Fig. 1b) was mounted in the reactor prior to its charging. In another case, the sensor represented two aligned and centered matrixes, the first consisting of 16 copper–constantan thermocouples 15 mm in diameter (4 × 4), built into a glass-textolite plate of thickness 0.3 mm, and the second being the matrix of electrochemical cells (4 × 4) for measuring electric conductivity. In the other case, the sensor represented a matrix of thermocouples (4 × 4) and a matrix of electrochemical probes for measuring the potential difference. The cell for measuring electric conductivity consists of two platinum electrodes 100 μm in diameter, spaced a distance of 2 mm apart. The electrochemical probes are installed into the glass-textolite plate of thickness 0.3 mm. As the tests showed, the given design does not affect the front propagation in the reactor. The reagents of "Ch" brand are colorless crystals 0.5-4.0 mm in size. They were ground in a ball mill, and thereafter 0.2 ± 0.05 mm fractions were sampled. Preliminarily prepared components were mixed in a mortar. When malonic acid was added gradually by portions to piperazine, mixture clotting was observed each time during 1-2 min, whereas when piperazine was added to malonic acid, the clotting was only observed on adding the first portion. The piperazine/malonic acid molar ratios were varied from 3/1 to 1/3. It can be assumed that the reaction products are specified by the state of malonic acid. At the mixing stage, a dense envelope of piperazine surrounds a particle of malonic acid. The prepared mixture was placed in the reactor, where the charge was compacted using a hydraulic press.

The dynamic experiments provide a unique possibility of studying high-rate phase, structural, and chemical transformations in condensed substances. The main difficulty is related to the short time of synthesis in the front. Therefore, we used a method based on measuring electric resistance of the test cell during the front passage. Electric conductivity is calculated taking

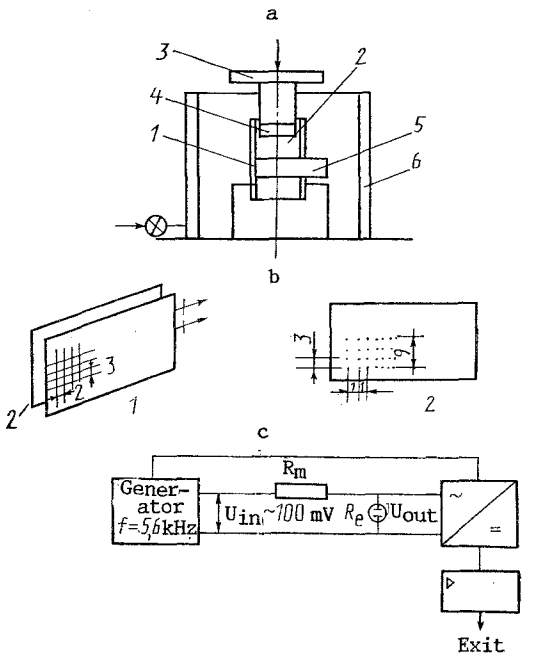

Fig. 1. Measuring system: a) reactor for studying combustion processes: 1) reactor wall; 2) charge; 3) pump; 4) ignition device; 5) sensor; 6) protective shield. b) Sensor: 1) thermocouple; 2) electrochemical matrix. c) electric-conductivity measuring circuit.

into account the geometric dimensions of the cell and the electrolytic modeling. At frequencies lower than 10^8 Hz, ohmic resistance for electrolyte solutions does not depend on frequency [16, 17]. In the general case, however, impedance can be a function of frequency, since it is determined not only by the ionic movement, but also by some other effects [16, 17]. The choice of the cell structure and the platinization of the electrodes dramatically weaken the influence of some of them. There are a number of factors involved in measuring electric conductivity, viz., parallel capacitance stipulated by dielectric properties of the solutions; capacitance of the double electric layer; and Faraday impedance associated with the electric charge transfer through the electrode–solution interface. The measurements were conducted at a frequency of 5.6 kHz. For such a frequency and for small dimensions of the cell, the conductor capacitance is negligible. The Faraday impedance was practically eliminated by a voltage of 100 mV applied to the cell. The method is based on measuring the voltage drop on the cell with stable current (Fig. 1c). The resistance R_m was chosen such that the current traversing the measuring circuit was stable. With the aid of synchronous rectification, the real part of the voltage drop on the cell R_e is separated. Then R_e can be determined by measuring U_{out} at the exit from the direct-conversion receiver, with U_{in} and R_m assigned.

Identifying the cell constant k via the electrolytic modeling, we calculate the specific electric conductivity

$$\lambda = k/R_e.$$

The measurement of the potential difference at various electrodes, in accordance with an electrochemical series, can give additional information on dynamic processes occurring in the front. The traditional method of voltage bucking due to the process dynamism is unsuitable here, since the speed of response in insufficient.

In measuring the potential difference we registered two quantities. The time variation of R_e was recorded by the technique outlined above. Afterwards the potential difference at the electrodes of different metals was measured with no outer sources. The sought quantity is found from the relation

$$U(t) = U_1(t)(R_e(t) + R_v)/R_v,$$

where $U_1(t)$ is the potential difference fixed by the voltmeter and R_v is the input resistance of the voltmeter.

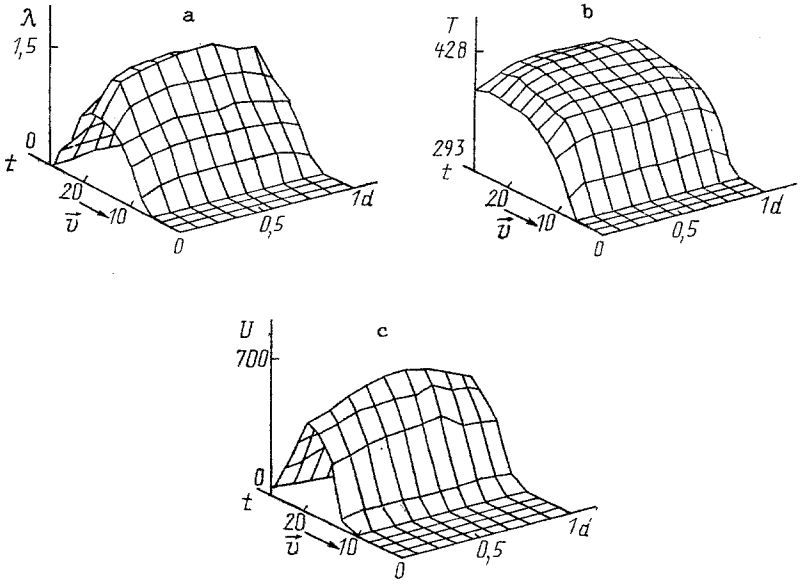

Fig. 2. Spatial–temporal distribution of electric conductivity (a), temperature (b), and potential difference in the combustion wave (c). λ, $\Omega^{-1} \cdot m^{-1}$; t, sec; U, mV; T, K.

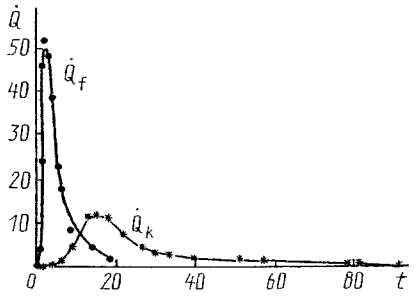

Fig. 3

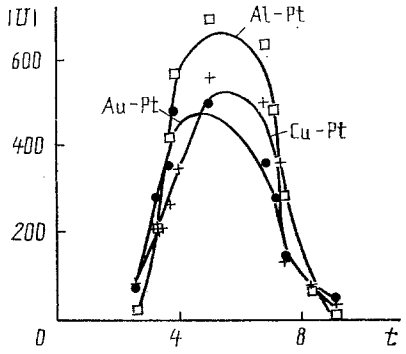

Fig. 4

Fig. 3. Heat release rates: $\dot{Q}_f$) in the synthesis wave; $\dot{Q}_k$) during synthesis in the calorimeter. $\dot{Q}$, kJ/(kg·sec).

Fig. 4. Variations in the potential difference modulus for different cells. |U|, mV.

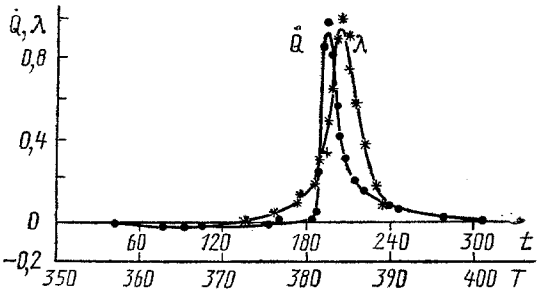

Fig. 5. Variations in heat release rate and in electric conductivity during synthesis in a calorimeter.

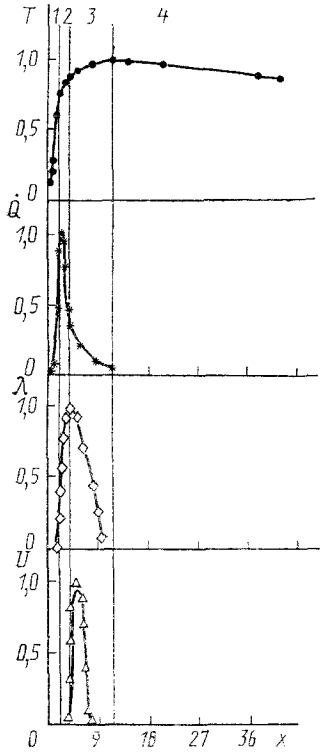

Fig. 6. Stages of transformations. x, mm.

The measurements of the constant for each cell and the method calibration were performed using the electrochemical modeling with solutions NaCl 0.1 M, 0.2 M, 0.5 M, 1 M, 2 M, and 4 M before each test. Statistical and calculated estimates of the method errors showed a relative error of 11% for measuring electric conductivity and 13-15% for measuring potential difference.

The processes proceeding in the front are fairly rapid (about 1 sec), while the number of sensors is great. Therefore, we developed methods for automated measurements on the basis of the peripheral computer of the IVK-6 SM-1300 set in the CAMAC standard. This unit allows the following comprehensive measurements:

spatial–temporal temperature distribution in the reactor;

spatial–temporal distribution of electric conductivity and potential difference.

Thermophysical Properties of the Objects Studied . To analyze kinetic regularities and thermal fields in the wave of the self-propagating synthesis, we defined the thermophysical properties of the original components and mixture. Tests conducted with a scanning calorimeter revealed that the exothermal effect for the stoichiometric mixture is Q = 250-270 kJ/kg. The results obtained in [1, 3] using differential thermal analysis give 242-260 kJ/kg. In measuring specific heat, the compression pressure was set up the same as for compacting in the cylindric reactor. The data obtained are approximated by the following relationship

$$C_p(T) = A + BT,$$

where $C_p(T)$ is the specific heat J/(kg·K) and T is the temperature, K.

The constants are presented in Table 2. The data on specific heat cover the range from 30°C up to the melting temperature of the components. In conformity with [18], for specific heat of the mixture of malonic acid and piperazine it is possible to write

$$C_p^{CM} = M_{MA} C_{pMA} + M_{PP} C_{pPP}.$$

The standard error of this relation for temperatures of 30-70°C is not larger than 7%. The measurements of thermal conductivity indicated that, within the range from 25°C up to the melting point, the following relation is fulfilled:

$$L(T, \rho) = A(1 + B(T - 300))(1 + C_\rho).$$

TABLE 2. Results of Measuring Specific Heat

Substance	A	$B \cdot 10^{-3}$	RMS deviation, %	Correlation factor, %
Malonic acid	0,22	4,32	4	86
Piperazine	—2,5	13,2	5	96
Synthesis product	0,045	4,53	6	87

TABLE 3. Results of Measuring Thermal Conductivity

Substances	A	$B \cdot 10^{-3}$	C	RMS deviation, %	Correlation factor, %
Malonic acid	0,095	2	2	5	86
Piperazine	0,48	13	—	6	80
Reaction product	0,103	1,6	1,02	5	85

For piperazine, variations with the compactness comprised less than 8%, which is smaller than the measurement errors. The constants for these substances are given in Table 3. Thermal conductivity for the mixture of malonic acid and piperazine at T = 25-50°C is assessed from the relation:

$$L = M_{\text{MA}} L_{\text{MA}} + M_{PP} L_{PP}.$$

The standard error of this relation in the range T = 25-50°C does not exceed 9%.

Discussion of the Results. *1. Dynamics of the Thermal Processes.* The front velocity in the conditions described equals 0.6 mm/sec. The maximal temperature in the reaction front is 155°C. This implies that both of the components in the wave are in a liquid phase. Figure 2 depicts a spatial–temporal evolution of temperature, electric conductivity, and potential difference fields, obtained using the suggested technique. In the near-wall region (of size about 3 mm), transverse temperature gradients are 20 K/cm, and the front curving across the cylinder radius is observed. When the reactor diameter doubles, the combustion rate increases by a factor of 1.5, whereas the radial gradients decrease; specifically, the temperature gradient falls to 5 K/sec, with the maximal front temperature invariable. This indicates the formation of an envelope, shielding the remaining charge from heat losses. When the mixture radius increases as compared to the inert layer (the reactor shell), the shielding layer gets thinner. According to [19, 20], the shielding envelope is characterized by a small transformation degree, whereas in the remaining charge adiabatic combustion is realized.

The equation describing the thermal processes in the established wave [2] can be written in the form

$$L/\rho/V^2 \partial^2 T/\partial t^2 - \rho C_p \partial T/\partial t + \dot{Q} = 0.$$

Integrating this relationship yields

$$Q(t) = C_p (T(t) - T_0) - L/\rho/V^2 \partial T/\partial t. \tag{1}$$

The specific heat and thermal conductivity of the original mixture as functions of the product quantity vary within 20-30%; therefore in the region of phase transitions we used the relations:

$$C_p = [C_p^{CM} + C_p^{PR}]/2,$$
$$L = [L^{CM} + L^{PR}]/2.$$

Integration of Eq. (1) results in the thermal effect in the combustion front equal to 280 kJ/kg. Figure 3 shows the relations for the heat release rate in the calorimeter and for that in the synthesis wave, computed from Eq. (1). Here the heat release rate and, hence, the chemical reaction rate are noticeably lower, and the time needed to obtain 30 mg of the product in a pellet of diameter 15 mm is 2-3 min. With the autowave mode, the product yield for 1 sec in a reactor of diameter 15 mm is 240-270 mg. Therefore, when one component, viz., piperazine, melts during self-propagating synthesis, only a new phase nucleation takes place.

2. Electrophysical Transformations. We discovered that the process is accompanied by a stepwise variation in the electric conductivity and by the origination of the potential difference at the electrodes of different materials. Figure 4 plots time variations in the potential difference modulus in the synthesis front for several electrochemical cells. In the tests we used electrodes made of Au–Pt, Cu–Pt, Al–Pt, Ni–Pt, Al–Cu, and Ni–Cu. The potential difference polarity and the signal amplitude relation are found to correlate with the electrochemical series for aqueous solutions. The time variation for electric conductivity is plotted in Fig. 2a. The maximal electric conductivity in the reaction front comprises 1.5 $\Omega^{-1} \cdot m^{-1}$ for the cell with Pt–Pt electrodes. Proceeding from these data and from the fact that carbonic acids form salts with ionic bonds [20], we may deduce that ionic conductivity originates. As a result of the reaction, the generation of an N–H ionic bond is the most probable [21]. Figure 5 shows the plots for heat release and electric conductivity in the calorimeter. Electric conductivity sharply increases in the zone where heat release commenced, at the temperatures corresponding to a liquid phase emergence. The peak of electric conductivity is linked with the number of charge carriers which, in turn, is governed not only by the amount of the liquid phase, but also by the presence of impurities (of malonic acid and the product). Of great significance in this case is the likelihood that local regions of the malonic acid melt on the order of grain sizes of the original components will appear.

3. Sequence of the Autowave Mode Stages. The executed tests disclosed that the variations in the electrophysical parameters occurring in the wave have a direct bearing on the phase, structural, and chemical transformations. Comparing the emergence of electrophysical phenomena with the temperatures of phase transitions for each component (Fig. 6) allows one to conclude that the transformation in the combustion wave proceeds by stages. Before the melting point ($T < 100°C$) of piperazine is attained, the so-called warmup zone exists, where the components are in a solid phase. The second region exists for $100 \leq T \leq 130°C$. In accordance with the figure, in this zone piperazine is molten, whereas malonic acid is solid. This region is characterized by the onset of heat release, by the origination and growth of electric conductivity, and by the initiation of a new phase (the synthesis product) nucleation.

In the third region ($130 \leq T \leq 155°C$), malonic acid melts, thus giving rise to a sudden increase in the formation rate of the new phase. The electric conductivity reaches a maximum by a temperature of 155°C, and afterwards falls together with heat release. As is clear from Figs. 4 and 6, the potential difference originates at the electrodes of different materials, i.e., the number of charge carriers in this region passes through a maximum. The fourth zone is the region of cooling, when the temperature passes through a maximum.

It must be noted that there is a qualitative difference between synthesis of powders of the same dispersivity occurring in the calorimeter and with the autowave mode. Self-propagating synthesis proceeds in two stages (the components melt in turn), whereas in the calorimeter the piperazine melting goes in one stage.

The proposed technique not only permits the investigation of structural transformations and kinetics of chemical interactions in the wave, but also opens up wide prospects for the process diagnostics during synthesis, carried out on an industrial scale.

NOTATION

M_{MA}, M_{PP}, mass fractions of malonic acid and piperazine in the mixture; L_{MA}, L_{PP}, thermal conductivities of malonic acid and piperazine; ρ, L, C_p, density, thermal conductivity, and specific heat of the charge; V, combustion rate; t, time; $\bar{Q}$, heat release rate; C_p^{PR}, L^{PR}, specific heat and thermal conductivity of the synthesis product; U, potential difference; λ, electric conductivity.

LITERATURE CITED

1. E. G. Klimchuk, G. M. Avetisyan, and A. G. Merzhanov, Dokl. Akad. Nauk SSSR, **311**, No. 5, 1161-1164 (1990).
2. A. G. Merzhanov, in: Physical Chemistry. Modern Problems [in Russian], Moscow (1983), pp. 6-44.
3. Joe Wong, E. M. Larson, J. B. Holt, et al., Science, **249**, 1406-1409 (1990).
4. A. G. Merzhanov, in: Combustion Processes in Chemical Technology and Metallurgy [in Russian], Chernogolovka (1975), pp. 5-28.
5. N. P. Novikov, I. P. Borovinskaya, and A. G. Merzhanov, in: Combustion Processes in Chemical Technology and Metallurgy [in Russian], Chernogolovka (1975), pp. 174-188.
6. V. I. Itin and Yu. S. Naiborodenko, High-Temperature Synthesis of Intermetallic Compounds [in Russian], Tomsk (1989).

7. A. A. Shidlovskii, Principles of Pyrotechnics [in Russian], Moscow (1973).
8. V. A. Assonov, Review of Foreign Industrial Explosives [in Russian], Moscow (1957).
9. L. V. Dubnov, N. S. Bakharevich, and A. I. Romanov, Industrial Explosives, 3rd ed. [in Russian], Moscow (1988).
10. K. K. Andreev, Thermal Decomposition and Combustion of Explosives [in Russian], Moscow (1966).
11. A. F. Belyaev, Combustion, Detonation, and Performance of an Explosion of Condensed Systems [in Russian], Moscow (1968).
12. A. G. Merzhanov, Z. P. Zhul'man, B. M. Khusid, et al., Topochemical Transformations in the Wave of an Exothermal Reaction of Organic Substances. Preprint No. 26 [in Russian], Heat and Mass Transfer Institute, Academy of Sciences of the Belorussian SSR, Minsk (1990).
13. E. G. Klimchuk, G. M. Avetisyan, and A. G. Merzhanov, Zh. Prikl. Khim., **63**, No. 6, 1436-1437 (1990).
14. E. G. Klimchuk and A. G. Merzhanov, Fiz. Goreniya Vzryva, **26**, No. 6, 104-108 (1990).
15. G. R. Desiraju, Crystal engineering. The design of organic solids. Materials science monographs 54. Elsevier (1989).
16. É. Eger and I. A. Zalkind (eds.), Measurement Methods in Electrochemistry, Vol. 2 [Russian translation], Moscow (1977).
17. É. Eger and I. A. Zalkind (eds.), Measurement Methods in Electrochemistry, Vol. 2 [Russian translation], Moscow (1977).
18. G. N. Dul'nev and Yu. P. Zarichnyak, Thermal Conductivity of Mixtures and Composites. Handbook [in Russian], Leningrad (1974).
19. S. S. Rybanin and S. A. Sobolev, Fiz. Goreniya Vzryva, **25**, No. 5, 16-25 (1989).
20. S. S. Rybanin and S. A. Sobolev, Dokl. Akad. Nauk SSSR, **268**, No. 6, 1394-1398 (1983).
21. B. P. Nikolskii (ed.), Handbook for a Chemist, Vol. 2 [in Russian], Moscow (1969).